

# Load-dependent inverted U-shaped connectivity of the default mode network in schizophrenia during a working-memory task: evidence from a replication functional MRI study

Feiwen Wang, MD\*; Chang Xi, PhD\*; Zhening Liu, MD, PhD; Mengjie Deng, MD; Wen Zhang, MD; Hengyi Cao, PhD; Jie Yang, PhD; Lena Palaniyappan, MD, PhD

**Background:** Working-memory deficit is associated with aberrant degree distribution of the brain connectome in schizophrenia. However, the brain neural mechanism underlying the degree redistribution pattern in schizophrenia is still uncertain. **Methods:** We examined the functional degree distribution of the connectome in 81 patients with schizophrenia and 77 healthy controls across different working-memory loads during an n-back task. We tested the associations between altered degree distribution and clinical symptoms, and we conducted functional connectivity analyses to investigate the neural mechanism underlying altered degree distribution. We repeated these analyses in a second independent data set of 96 participants. In the second data set, we employed machine-learning analysis to study whether the degree distribution pattern of one data set could be used to discriminate between patients with schizophrenia and controls in the other data set. **Results:** Patients with schizophrenia showed decreased centrality in the dorsal posterior cingulate cortex (dPCC) for the “2-back versus 0-back” contrast compared to healthy controls. The dPCC centrality pattern across all working-memory loads was an inverted U shape, with a left shift of this pattern in patients with schizophrenia. This reduced centrality was correlated with the severity of delusions and related to reduced functional connectivity between the dPCC and the dorsal precuneus. We replicated these results with the second data set, and the machine-learning analyses achieved an accuracy level of 71%. **Limitations:** We used a limited n-back paradigm that precluded the examination of higher working-memory loads. **Conclusion:** Schizophrenia is characterized by a load-dependent reduction of centrality in the dPCC, related to the severity of delusions. We suggest that restoring dPCC centrality in the presence of cognitive demands might have a therapeutic effect on persistent delusions in people with schizophrenia.

## Introduction

Working-memory deficit — the failure to represent, maintain and update information in a short period of time — is a key feature of neurocognitive deficit in schizophrenia.<sup>1</sup> It emerges in the prodromal stage, continues in the psychotic phase and persists even after symptomatic remission, resulting in a life-long cognitive burden.<sup>2</sup> This working-memory deficit appears to play a role in recurrences and relapses, and to impede functional recovery in schizophrenia; it is also associated with persistent clinical symptoms.<sup>3</sup> Uncovering the elusive neurophysiological basis for such working-memory deficits might provide novel interventional targets for disease-modifying, procognitive interventions in people with schizophrenia.

The human brain has a well-replicated pattern of coordination among large-scale networks when it is performing tasks that place demands on working memory. Such coordination involves activation of the nodes of the central executive network and the salience network, and deactivation of the default mode network.<sup>4,5</sup> The degree of this triple-network coordination varies with participants’ task engagement, and with performance metrics. In general, inverted U-shaped neural recruitment of the nodes of the central executive network,<sup>6</sup> along with a linear load-related suppression of the default mode network, has been noted in healthy participants in relation to superior performance on tasks with working-memory demands.<sup>7</sup>

Compared to healthy participants, patients with schizophrenia show 2 distinct, interrelated patterns of load-related

**Correspondence to:** J. Yang, Department of Psychiatry, Second Xiangya Hospital of Central South University, Changsha 410011, Hunan, China; yang0826@csu.edu.cn

\*These authors contributed equally to this publication.

Submitted Mar. 24, 2022; Revised Jun. 28, 2022; Revised Jul. 30, 2022; Accepted Aug. 5, 2022

**Cite as:** *J Psychiatry Neurosci* 2022 September 27;47(5). doi: 10.1503/jpn.220053

abnormalities when they perform working-memory tasks. First, patients show a blunting<sup>8</sup> or a leftward shift<sup>9–11</sup> of the inverted U–shape relationship between working-memory load and recruitment of the nodes of the central executive network and salience network. Second, patients show a lack of load-dependent suppression of the default mode network,<sup>12</sup> indicating higher activation<sup>13–15</sup> in patients with schizophrenia relative to healthy controls; this hyperactivation of the default mode network is associated with working-memory impairment in patients with schizophrenia.<sup>15,16</sup>

This pattern of “default mode network intrusion” during working-memory tasks is not specific to established schizophrenia:<sup>17</sup> it appears even in those at risk<sup>12</sup> and in the first-episode phase. However, when sufficient task engagement and performance is achieved,<sup>11,18</sup> excess load-related deactivation of the default mode network has also been reported in patients with schizophrenia.<sup>11,18,19</sup> These findings indicate neural inefficiency (or “early peaking”) when handling cognitive load in the neurocognitive networks. When the demands of the working-memory task arise, patients with schizophrenia disproportionately require higher recruitment of the central executive network and the salience network — and higher suppression of the default mode network — to meet performance requirements,<sup>9–11,18,19</sup> but as they fail to sustain these neural resources at higher working-memory loads, working-memory dysfunction might become apparent.

In addition to inefficient regional activation or deactivation, aberrant brain connectivity in schizophrenia also contributes to working-memory deficits. At the global connectome level, we have shown that whole-brain connectivity becomes more segregated in patients with schizophrenia, with a more homogeneous redistribution of hubs in the presence of working-memory demand.<sup>20</sup> At the network level, previous studies have indicated that the major posterior hubs of the default mode network might share neural resources with the central executive network in healthy participants,<sup>15,21</sup> and that this connectivity might be reduced in schizophrenia.<sup>15,22</sup>

At present, we do not know whether cognitive load has specific effects on the global connectivity of hub regions in patients with schizophrenia. In particular, it is unclear whether the left shift of the inverted U–shaped model of activation in patients with schizophrenia also affects the connectivity patterns relevant to the handling of cognitive load.

Although working-memory deficits are seen as enduring features of schizophrenia, patients’ tendency to experience positive symptoms appears to be related to a reduced ability to handle higher cognitive loads.<sup>23</sup> Stressful milieux that often precede relapses affect working-memory capacity,<sup>24</sup> and might operate through cognitive deficits to provoke a recurrence of positive symptoms. Social and emotional stimuli become more distracting when patients’ working-memory loads are high.<sup>25</sup> At present, we do not know whether the brain dysconnectivity related to working-memory load also relates to the clinical symptoms of schizophrenia, especially to positive symptoms.

Graph theory is a powerful tool for investigating the topological characteristics of the brain network (i.e., the configuration of relationships among connections).<sup>26</sup> In this approach, brain networks are depicted as graphs of nodes (brain regions) connected by edges (the functional connectivity between regions). This framework allows abstract and complex relationships to be visually traceable, mathematically characterized and computed at an individual level for statistical inferences.

The degree centrality (DC) and the eigenvector centrality (EC) of a node in a graph (in this case, a brain region) represent the relative importance of that region for sustaining the overall connectedness of the whole brain. Degree centrality reflects the number of instantaneous functional connections of a particular region with other brain regions (targets), irrespective of the connectedness of the target regions themselves. Eigenvector centrality considers the quality of the connections, assigning a higher weight to those with highly connected targets (e.g., brain hubs). If we consider a simple model of information transmission across the brain that depends only on the degree of connectivity of a region, then regions with high DC are likely to have wider reach (i.e., many direct connections), and those with high EC are likely to have wider influence (i.e., connections with those regions are likely to be connected to many other regions and thus have more indirect connections).

In the present study, we used DC and EC indices to investigate the voxel-wise effect of working-memory loads on the functional connectome in 2 independent patient samples, using an n-back task. We hypothesized that patients with schizophrenia and healthy controls would exhibit load-dependent centrality changes, most prominently in the default mode network. We also hypothesized that altered centrality patterns captured by EC and DC metrics would relate to the positive symptoms of schizophrenia. Last, we tested whether the centrality pattern carried sufficient illness-specific information to discriminate between the patterns observed in patients with schizophrenia and those observed in healthy controls.

## Methods

### *Participants*

The study cohort comprised a discovery data set (data set 1; 105 patients and 91 healthy controls) and a second independent data set (data set 2; 56 patients and 55 healthy controls). All participants were right-handed native Chinese speakers, and they provided written informed consent for participation in the protocol, which was approved by the medical ethics committee of the Second Xiangya Hospital, Central South University.

We performed psychiatric evaluations in all patients with schizophrenia. We assessed clinical symptoms using the Scale for the Assessment of Positive Symptoms (SAPS)<sup>27</sup> and the Scale for the Assessment of Negative Symptoms (SANS).<sup>28</sup> We assessed cognitive function in all study participants using the information and digit–symbol subscales of the Wechsler Adult Intelligence Scale–Chinese Revised (WAIS–CR).<sup>29</sup>

Detailed descriptions of all participants are provided in Appendix 1, supplementary material S1, available at [www.jpnp.ca/lookup/doi/10.1503/jpn.220053/tab-related-content](http://www.jpnp.ca/lookup/doi/10.1503/jpn.220053/tab-related-content).

### *MRI data acquisition and preprocessing*

We acquired data set 1 on a Philips Achieva 3 T scanner and data set 2 on a Siemens Allegra 3 T scanner. Scanning factors differed slightly (Appendix 1, supplementary material S2), and we took these differences into account during preprocessing.

We accomplished data preprocessing using the DPABI toolbox.<sup>30</sup> First, we dropped 2 volumes of data set 1 and 5 volumes of data set 2 to achieve stability of magnetic saturation. The remaining 248 volumes for each participant entered the following preprocessing steps: slice timing correction, motion realignment, smoothing and spatial normalization to Montreal Neurological Institute (MNI) space. Nuisance covariates (including 12 head-motion parameters, white matter and ventricle signals) were regressed out. We preserved the global signal because of the possibility of illness-related variance in global signals.<sup>31</sup> We interpolated displaced volumes using nearest-neighbour interpolation (frame-wise displacement > 0.5 mm).<sup>32</sup> Exclusion criteria included head motion greater than 2.5° rotation or 2.5 mm translation in any direction, and failure of functional MRI (fMRI) data normalization and registration to MNI space because of acquisition errors.

After quality control, 254 participants were included in the final analysis (data set 1: 81 patients with schizophrenia and 77 healthy controls; data set 2: 46 patients with schizophrenia and 50 healthy controls). We found no significant differences in the total number of displaced volumes that underwent interpolation in patients versus controls across the 2 data sets (mean ± standard deviation; data set 1: patients with schizophrenia = 15.4 ± 18.2, healthy controls = 13.0 ± 15.6,  $p = 0.36$ ; data set 2: patients = 7.3 ± 9.73, healthy controls = 4.7 ± 7.53,  $p = 0.14$ ).

### *Calculation of degree centrality and eigenvector centrality*

The working-memory paradigm comprised 2 load conditions (0-back and 2-back); a detailed description of this paradigm is provided in Appendix 1, supplementary material S3. Before calculating the DC and EC maps, we reorganized the preprocessed fMRI data. For each participant, we separately concatenated the fMRI volumes obtained under the 8 blocks of the rest condition, the 4 blocks of the 0-back load and the 4 blocks of the 2-back load, and we generated these 3 modes of fMRI data with 80 volumes each.

We conducted the voxel-wise DC and EC value calculations using DPABI software<sup>30</sup> and the FastECM toolbox ([github.com/amwink/bias/tree/master/matlab/fastECM](https://github.com/amwink/bias/tree/master/matlab/fastECM)), respectively. Before calculating centrality maps, we used a mask to exclude white matter from the fMRI data; the whole-brain voxel-based centrality maps were calculated based on grey matter only. Voxel-wise DC indicates the number of instantaneous functional connections of a voxel. Voxel-wise EC attributes a value to each voxel in the brain: a larger value indicates that a voxel is strongly correlated with many other nodes, which are themselves central in the

network. Calculation details are presented in Appendix 1, supplementary material S4. We processed the above manipulations for the resting condition and the 0-back and 2-back loads, and we generated 3 types of centrality maps for statistical analysis.

### *Statistical analysis*

We used SPSS statistical software (version 22) to compare demographic and clinical characteristics and working-memory task performance across groups. We analyzed differences in age, years of education, accuracy and response time under the 0-back and 2-back loads using 2-sample  $t$  tests. We analyzed sex differences using  $\chi^2$  tests.

We performed statistical analysis of the fMRI data using Statistical Parametric Mapping 12 software ([www.fil.ion.ucl.ac.uk/spm](http://www.fil.ion.ucl.ac.uk/spm)). First, we used subtraction in the DC maps to generate 3 types of contrasts: 0-back versus rest, 2-back versus rest and 2-back versus 0-back. Then, we separately submitted the generated contrast maps for each participant to group analysis using 2-sample  $t$  tests to test for group differences, using sex, age and years of education as covariates. We corrected all data for multiple comparisons using false discovery rate correction at  $p < 0.05$  and cluster  $k > 15$ .

### *Exploratory analysis*

#### **Correlation analysis**

We extracted the centrality values of the regions that showed group differences and conducted Pearson correlation analysis between these centrality values and cognitive measures and clinical symptoms. We further explored which subcomponents of the relevant clinical scores were tonically varied with altered centrality values.

#### **Machine-learning analysis**

We extracted the DC and EC values of regions that showed significant group-related differences, and we conducted pattern recognition analysis using the support-vector machine (SVM) approach proposed by Cortes and Vapnik<sup>33</sup> and implemented using the libsvm toolkit ([www.csie.ntu.edu.tw/~cjlin/libsvm/](http://www.csie.ntu.edu.tw/~cjlin/libsvm/)). We set the kernel function of the SVM as the sigmoid type; all other related parameters used default settings as a trade-off between training error and generalizability ( $c = 10$ ;  $g = 1/\text{number of all features}$ ;  $\text{coef} = 0$ ), in line with our previous work.<sup>34</sup> We used data set 1 to train the classifier, and data set 2 as the testing sample. We calculated the average prediction accuracy, the area under the curve, the true positive rate for schizophrenia and the true positive rate for healthy controls to evaluate the performance of the classifier.

#### **Functional connectivity analysis**

Because the voxel-wise centrality index reflects the total degree of functional connectivity between a certain voxel and all other voxels of the brain, we performed a functional connectivity analysis to locate areas with aberrant functional connectivity that drove alterations in the centrality pattern.

## Results

### Participant characteristics

Demographic and clinical findings from data set 1 are presented in Table 1. Patients with schizophrenia were somewhat older than the healthy controls ( $t = 2.07, p = 0.040$ ), and their years of education were notably lower ( $t = -6.5, p < 0.001$ ). As expected, the working-memory performance of the patients across all loads was worse than that of the healthy controls, with a longer response time (0-back:  $t = 4.2, p < 0.001$ ; 2-back:  $t = 2.8, p = 0.006$ ) and lower accuracy (0-back:  $t = -4.3, p < 0.001$ ; 2-back:  $t = -6.7, p < 0.001$ ). Patients also scored lower on the Wechsler Adult Intelligence Scale–Chinese Revised information ( $t = -4.4, p < 0.001$ ) and digit–symbol ( $t = -10.7, p < 0.001$ ) subscales compared to healthy controls.

Group differences in data set 2 were generally consistent with those in data set 1; details are provided in Appendix 1, Table S1.

### Centrality maps

In the “2-back versus rest” and “0-back versus rest” contrasts, no brain areas showed group differences in the centrality index. However, in the “2-back versus 0-back” contrast, patients

with schizophrenia showed a strong reduction in DC (peak MNI coordinates  $x, y, z = 0, -39, 33$ ; cluster size = 19;  $t = -6.1$ ; Cohen  $d = 0.98$ ; Figure 1) and EC (peak MNI coordinates  $x, y, z = -3, -39, 33$ ; cluster size = 15;  $t = -5.3$ ; Cohen  $d = 0.85$ ; Figure 1) in the dorsal posterior cingulate cortex (dPCC) compared to healthy controls. We observed significant differences in the centrality of the dPCC when we compared female patients with male patients (DC:  $p = 0.9$ ; EC:  $p = 0.65$ ).

We extracted the centrality values for the dPCC and fitted them to the changing working-memory loads in the patient group, reflecting an inverted U-shaped model. We observed the lowest centrality value in the rest condition (DC =  $0.18 \pm 0.71$ ; EC =  $0.11 \pm 0.87$ ) and the highest centrality value for the 0-back load (DC =  $0.60 \pm 0.67$ ; EC =  $0.5 \pm 0.68$ ), but a notable drop again for the 2-back load (DC =  $0.30 \pm 0.78$ ; EC =  $0.31 \pm 0.80$ ). In contrast, healthy controls showed a tonic positive correlation between dPCC centrality and working-memory load (rest: DC =  $0.18 \pm 0.73$ , EC =  $0.26 \pm 0.77$ ; 0-back: DC =  $0.39 \pm 0.72$ , EC =  $0.37 \pm 0.73$ ; 2-back: DC =  $0.75 \pm 0.55$ , EC =  $0.73 \pm 0.53$ ). These findings were suggestive of a left shift of the summit location of the centrality value of the dPCC in patients with schizophrenia compared to healthy controls, leading to the emergence of significant group differences in the “2-back versus 0-back” contrast as reported above. Details are provided in Figure 2.

**Table 1: Participant demographic and clinical characteristics, data set 1**

| Item  | Patients with schizophrenia*<br><i>n</i> = 81 | Healthy controls*<br><i>n</i> = 77 | <i>t</i> / $\chi^2$ | <i>p</i> value |
|---|---|------------------------------------|---------------------|----------------|
| Age, yr   | 24.46 ± 5.62                                  | 22.87 ± 3.90                       | 2.069               | 0.040‡         |
| Sex, M/F  | 51/30   | 37/40                              | 3.557               | 0.06           |
| Education, yr                                     | 11.65 ± 2.83                                  | 14.2 ± 2.09                        | -6.502              | < 0.001‡       |
| Onset age, yr                                     | 22.58 ± 5.39                                  | NA                                 | NA                  | NA             |
| Illness duration, mo                              | 22.93 ± 27.45                                 | NA                                 | NA                  | NA             |
| Treatment duration, mo                            | 7.53 ± 13.62                                  | NA                                 | NA                  | NA             |
| Total dosage, mg/d†                               | 378 ± 238                                     | NA                                 | NA                  | NA             |
| Scale for Assessment of Positive Symptoms         |   |                                    |                     |                |
| Total score                                       | 19.34 ± 14.43                                 | NA                                 | NA                  | NA             |
| Hallucination score                               | 4.16 ± 5.61                                   | NA                                 | NA                  | NA             |
| Delusion score                                    | 8.74 ± 7.27                                   | NA                                 | NA                  | NA             |
| Bizarre behaviour score                           | 3.27 ± 3.99                                   | NA                                 | NA                  | NA             |
| Positive formal thought disorder score            | 3.01 ± 4.49                                   | NA                                 | NA                  | NA             |
| Scale for Assessment of Negative Symptoms         |   |                                    |                     |                |
| Total score                                       | 35.03 ± 27.05                                 | NA                                 | NA                  | NA             |
| Wechsler Adult Intelligence Scale–Chinese Revised |   |                                    |                     |                |
| Information subscale score                        | 16.70 ± 4.70                                  | 20.96 ± 4.86                       | -4.396              | < 0.001‡       |
| Digit–symbol subscale score                       | 63.21 ± 12.86                                 | 90.91 ± 12.73                      | -10.676             | < 0.001‡       |
| 0-back load                                       |   |                                    |                     |                |
| Accuracy, %                                       | 78 ± 23                                       | 92 ± 15                            | -4.332              | < 0.001‡       |
| Response time, ms                                 | 570 ± 142                                     | 486 ± 93                           | 4.194               | < 0.001‡       |
| 2-back load                                       |   |                                    |                     |                |
| Accuracy, %                                       | 48 ± 24                                       | 74 ± 19                            | -6.718              | < 0.001‡       |
| Response time, ms                                 | 725 ± 176                                     | 649 ± 141                          | 2.805               | 0.006‡         |

NA = not applicable.

\*Values are mean ± standard deviation, unless otherwise indicated.

†Antipsychotic dosage refers to dose equivalents for chlorpromazine calculated using the classical mean dose method.<sup>35</sup>

‡Significant at  $p < 0.05$ .

We used the subregion that showed significant group differences under the “2-back versus 0-back” contrast in data set 1 as a mask, and conducted the same analyses for data set 2. Findings were consistent with those for data set 1 (Appendix 1, supplementary material S5 and Figure S2).

Differences between patients with schizophrenia and healthy controls in the conventional task activation analysis using the 0-back load, 2-back load and “2-back versus 0-back” contrast are shown in Appendix 1, Figure S3.

### Exploratory analysis

#### Correlation analysis

After pooling samples from the 2 data sets and extracting the centrality value of the dPCC from the “2-back versus 0-back” contrast, we observed that both the DC ( $r = -0.21$ ,  $p = 0.024$ ) and EC ( $r = -0.275$ ,  $p = 0.002$ ) values were negatively correlated with scores on the Scale for Assessment of Positive Symptoms (SAPS).

We divided the full SAPS scale into 4 component scales (hallucination, items 1–7; delusion, items 8–20; bizarre behaviour, items 21–25; and positive formal thought disorder, items 26–34), and found that the negative relationship between centrality value and SAPS score was driven

specifically by delusions (DC:  $r = -0.19$ ,  $p = 0.036$ ; EC:  $r = -0.26$ ,  $p = 0.004$ ; Figure 3).

We found no significant associations between the centrality value of the dPCC from the “2-back versus 0-back” contrast and working-memory performance measures or medication dose in either data set (Appendix 1, Table S2C). We also found no significant associations between working-memory performance and medication dose (Appendix 1, Table S3). Detailed findings for the correlations between DC and EC values in the dPCC and working-memory performance and clinical symptoms are provided in Appendix 1, Tables S2 and S4.

#### Machine-learning analysis

We extracted the voxel-wise DCs and ECs in the dPCC that showed significant group-related differences in the “2-back versus 0-back” contrast as features (total of 34 features: 19 voxels from the DC maps and 15 voxels from the EC maps). These features then entered machine-learning analysis. Using data set 1 as the training data set and data set 2 as the sample set, we achieved classification results with average accuracy (70.53%), area under the curve (0.71), true positive rate for schizophrenia (76.09%) and true positive rate for healthy controls (65.31%). The accompanying receiver operator characteristic plot is shown in Appendix 1, Figure S4.

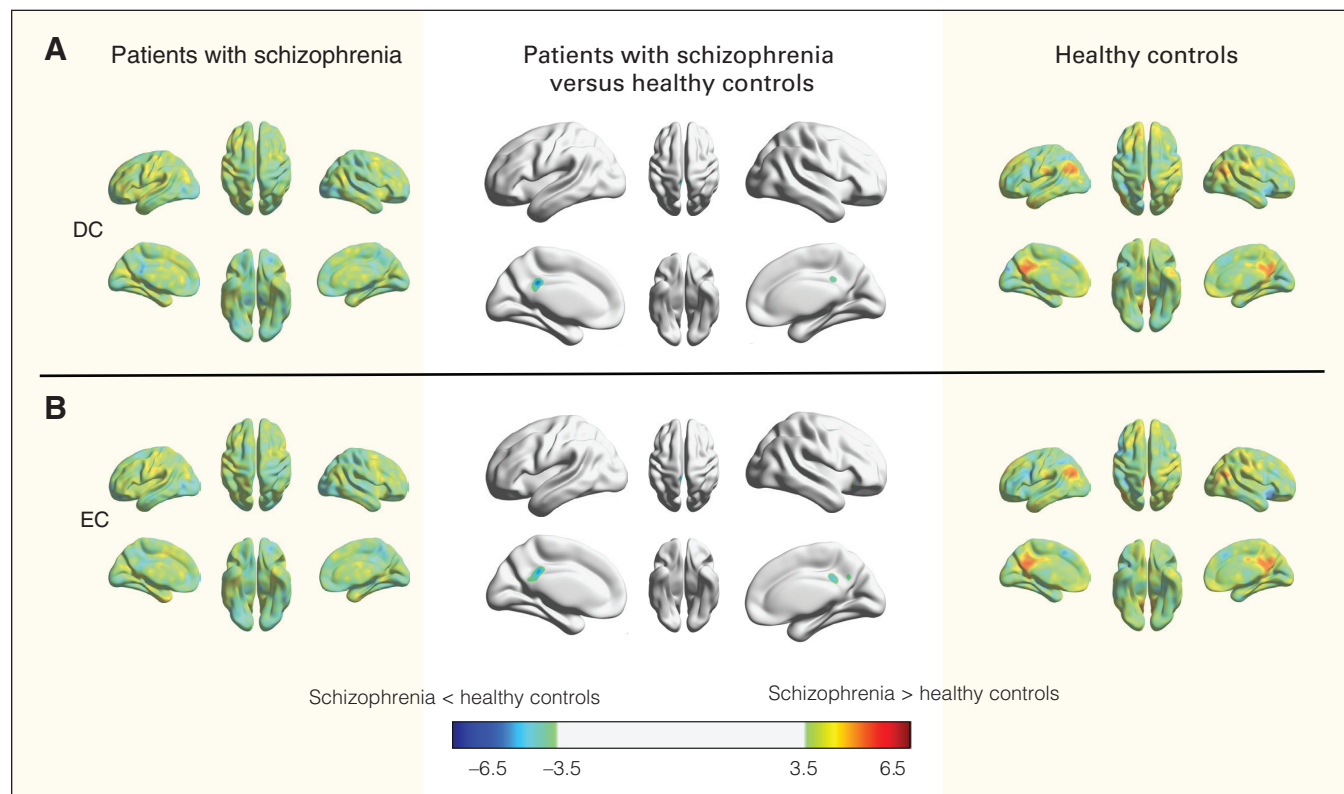


**Figure 1:** Centrality differences between patients with schizophrenia and healthy controls. (A) Patients with schizophrenia showed decreased degree centrality in the dorsal cingulate cortex under the “2-back versus 0-back” contrast compared to healthy controls. (B) Patients with schizophrenia showed decreased eigenvector centrality in the dorsal cingulate cortex under the “2-back versus 0-back” contrast compared with healthy controls. DC = degree centrality; EC = eigenvector centrality.

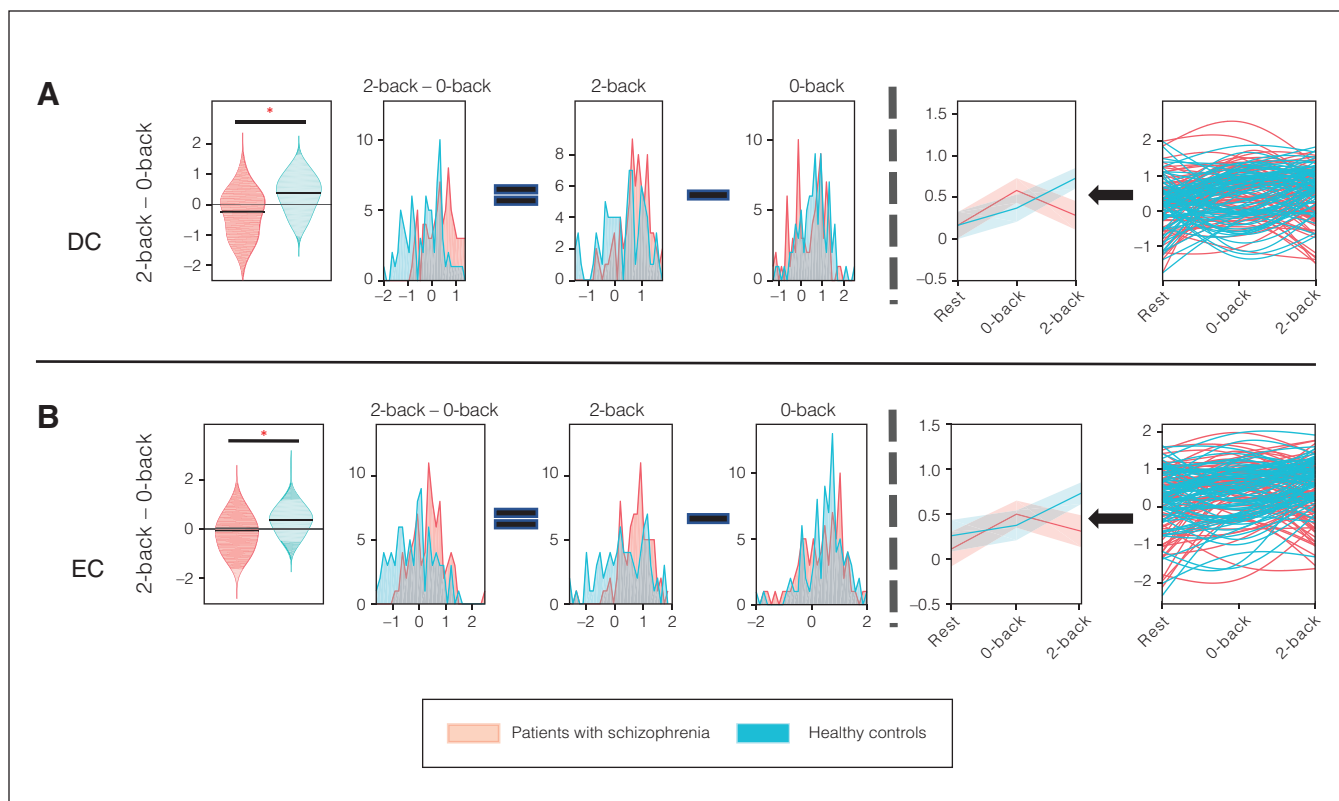


**Figure 2:** Centrality of the dorsal cingulate cortex across all working-memory loads. Diagrams in the left panel illustrate the centrality distribution of the dPCC during the 0-back and 2-back loads, and the “2-back versus 0-back” contrast; the horizontal axis represents the centrality value of the dPCC, and the vertical axis represents the number of participants. Diagrams in the right panel illustrate the centrality value of the dPCC across different working-memory loads. The horizontal axis represents working-memory loads and the vertical axis represents the centrality value of the dPCC. (A) Patients with schizophrenia showed decreased degree centrality in the dPCC in the “2-back versus 0-back” contrast compared to healthy controls, and their centrality pattern across all working-memory loads fit an inverted U-shaped pattern. (B) Patients with schizophrenia showed decreased eigenvector centrality in the dPCC in the “2-back versus 0-back” contrast compared to healthy controls, and their centrality pattern across all working-memory loads fit an inverted U-shaped pattern. DC = degree centrality; dPCC = dorsal posterior cingulate cortex; EC = eigenvector centrality.

### Functional connectivity analysis

We selected the detected dPCC area (cluster size = 19) as the seed and performed whole-brain functional connectivity analysis using data set 1. Under the “2-back versus 0-back” contrast, we observed decreased functional connectivity between the seed and the dorsal precuneus ( $t = -6.24$ , Cohen  $d = 0.99$ ), the right middle occipital gyrus ( $t = -5.82$ , Cohen  $d = 0.93$ ) and the right superior temporal gyrus ( $t = -5.51$ , Cohen  $d = 0.88$ ) in patients with schizophrenia compared to healthy controls; no areas showed increased functional connectivity with the dPCC in patients with schizophrenia. Details are provided in Figure 3 and Table 2.

We extracted the statistic map of the functional connectivity analysis from data set 1 as a mask and conducted the same functional connectivity analysis using data set 2; findings were consistent with those of data set 1 (details in Appendix 1, supplementary material S6).

Similar to the DC of the dPCC, the functional connectivity of the dPCC and regions with reduced connectivity in patients with schizophrenia also fit an inverted U-shaped pattern in both data sets (Appendix 1, Tables S5 and S6, and Figures S5 and S6).

### Discussion

The current study aimed to investigate voxel-wise centrality pattern changes across all working-memory loads in a large sample of patients with schizophrenia using DC and EC indices; we replicated our analysis in a second independent sample with different scanning parameters. We report 3 main findings here. First, compared to healthy controls, patients with schizophrenia displayed decreased centrality in the dPCC with increased cognitive load, and this load-dependent reduction in dPCC connectivity was related to the severity of positive symptoms — especially delusions. Second, the load-related centrality changes in dPCC connectivity fit an inverted U-shaped model, with a left shift of distribution in patients with schizophrenia compared to healthy controls. Third, reduced functional connectivity of the precuneus, middle occipital gyrus and superior temporal gyrus with the dPCC contributed to the load-dependent reduction in dPCC centrality in patients with schizophrenia.

We observed an inverted U-shaped relationship between the centrality of the dPCC and working-memory loads in

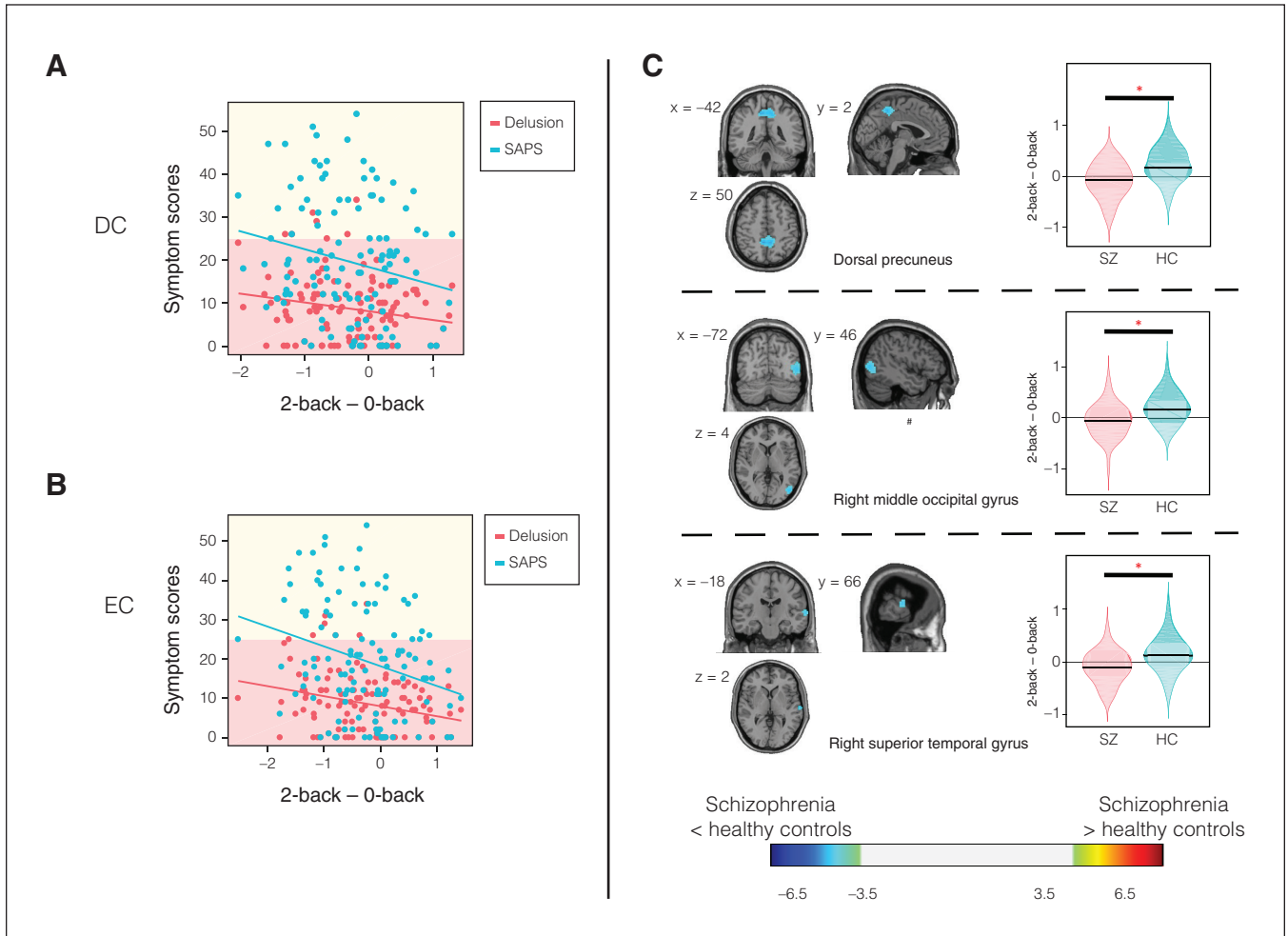


**Figure 3:** Exploratory analysis. (A) The degree centrality value in the dorsal cingulate cortex was negatively correlated with SAPS ( $r = -0.21$ ,  $p = 0.024$ ) and delusion ( $r = -0.19$ ,  $p = 0.036$ ) scores. (B) The eigenvector centrality value in the dorsal cingulate cortex was negatively correlated with SAPS ( $r = -0.275$ ,  $p = 0.002$ ) and delusion ( $r = -0.26$ ,  $p = 0.004$ ) scores. (C) Brain regions showing significant group differences in functional connectivity compared to the dorsal cingulate cortex under the “2-back versus 0-back” contrast. DC = degree centrality; EC = eigenvector centrality; HC = healthy control; SAPS = Scale for Assessment of Positive Symptoms; SZ = schizophrenia.

**Table 2: Regions that showed abnormal connectivity with the dorsal posterior cingulate cortex in patients with schizophrenia in the “2-back versus 0-back” contrast**

| Brain regions                                  | Cluster size, voxels | Peak coordinates<br>x, y, z | t     | Cohen d |
|--|----------------------|-----------------------------|-------|---------|
| Patients with schizophrenia < healthy controls |                      |                             |       |         |
| Dorsal precuneus                               | 178                  | 6, -45, 51                  | -6.24 | 0.9995  |
| Right middle occipital gyrus                   | 102                  | 48, -75, 6                  | -5.82 | 0.9322  |
| Right superior temporal gyrus                  | 22                   | 66, -18, 3                  | -5.51 | 0.8826  |
| Patients with schizophrenia > healthy controls |                      |                             |       |         |
| Not available                                  |                      |                             |       |         |

the patient group in data set 1; we had similar findings in data set 2. Many previous studies have suggested that the dPCC is a crucial component of the default mode network,<sup>36</sup> and a common hub shared with the default mode network and other large-scale networks,<sup>21</sup> assisting in

resource allocation and outcomes during task performance. The dPCC also participates in sharing attentional focus between the default mode network and the frontoparietal network, showing a high degree of connectivity with attention networks at rest.<sup>37,38</sup>

We did not observe an inverted U pattern of connectivity for the dPCC in healthy controls. In nodes of the default mode network (unlike in task-positive nodes such as the lateral prefrontal regions<sup>39</sup>), the most often-reported relationship between deactivation and working-memory performance to date has been a linear one (also seen in our activation contrasts presented in Appendix 1, Figure S3). In healthy controls, higher loads may be required for the same pattern to emerge as is seen in patients.<sup>9</sup>

The reduced load-dependent connectivity of the dPCC in schizophrenia raises an important question about the physiologic role of the dPCC in working-memory tasks. The conventional notion that the default mode network is a task-negative network that “distracts” from task performance is increasingly being challenged.<sup>40–43</sup> Thus, when demands on working-memory capacity increase, task-related engagement of certain segments of the default mode network may be required to maintain task performance.

In people with schizophrenia, several observations support a role for failed default mode network suppression in relation to reduced performance during working-memory tasks,<sup>13–15</sup> but excess default mode network deactivation compared to healthy controls occurs when performance is optimal.<sup>11,18,19</sup> In the present study, we noted a load-dependent reduction in the centrality of the dPCC and in its connectivity with other regions of the default mode network (e.g., the precuneus) in conjunction with reduced performance in patients with schizophrenia compared to healthy controls. This occurred despite a notable load-dependent reduction in deactivation (or nonsuppression) of the default mode network in general and the dPCC in particular in patients with schizophrenia. As well, the important role of the cingulate cortex in emotion has been proposed in previous theories,<sup>44</sup> and as part of the limbic system, the cingulate cortex plays complex roles in the emotional and memory domains.<sup>45</sup> Reduced load-dependent connectivity of the dPCC in people with schizophrenia might be also related to frustration (or weakening of efforts) when facing higher cognitive demands. Together, reduced centrality and insufficient suppression indicate a failure of efficient load-dependent contribution from the default mode network to ongoing demands of the working-memory task in people with schizophrenia.

Our results indicate that load-dependent loss of dPCC prominence in people with schizophrenia likely plays an important role in the mechanism of delusions. Although any single brain region is unlikely to play a causal role in the formation and maintenance of delusions, reduced centrality of the default mode network (dPCC) during a working-memory task in patients most affected by delusions might reflect a role of failed information transmission in the severity of delusions. In particular, social cues that present higher cognitive demands might induce a failed integration of brain regions centered in the default mode network, abetting delusional features.<sup>46,47</sup> Thus, when they face increased cognitive demands, people with schizophrenia may be unable to efficiently marshal neural resources centered on the default mode network to aid in information processing, arriving at or resisting the revision of incorrigible beliefs. Given the lack of further decision-making experiments or social cognition tasks in the present study, we call for future studies to test these speculations.

The reduction in dPCC centrality that we observed was related mainly to decreased functional connectivity with the dorsal anterior and central precuneus. The anterior dorsal precuneus has strong functional connectivity with the sensorimotor cortex,<sup>48,49</sup> and it has been suggested as a region of the sensorimotor network. The dorsal central precuneus is a cognitive-associative area connected with the frontoparietal and attention networks.<sup>48,49</sup> Other areas with significant functional connectivity differences, including the middle occipital gyrus<sup>50</sup> and superior temporal gyrus,<sup>51</sup> are related to visual or auditory function, which belong to the sensory system. In the context of the resource-allocation function of the dPCC during task performance,<sup>21</sup> our findings may demonstrate that patients inefficiently source sensorimotor contributions, leading to the working-memory deficits we observed.

### Limitations

Our study had numerous strengths and some limitations. We replicated our observations in a second independent data set, irrespective of differences in age of onset in data set 2. Nonetheless, we used a limited n-back paradigm that precluded examination of the parametric effect of higher working-memory loads (a contrast from Thomas and colleagues<sup>9</sup>). Second, all patients with schizophrenia were taking antipsychotic medications, and this might have influenced some of our findings, although we did not observe a correlation between total antipsychotic dose and working-memory performance (Appendix 1, Table S3). Third, the patients with schizophrenia in the present study had fewer years of education than the healthy controls, and previous studies have demonstrated that this factor influences the neural mechanisms of working-memory performance. We adjusted for this influence by using education level as a covariate in statistical analyses, but nonlinear effects might still be relevant. Finally, although our study was powered to demonstrate group differences in centrality distributions, the variance in working-memory performance was insufficient to uncover correlations between task accuracy and connectivity; this factor might explain the lack of expected correlation between dPCC centrality and working-memory metrics (Appendix 1, Table S4). Clinical samples with higher-performing patients and targeted recruitment of slower and more inaccurately performing healthy participants will be needed to avoid type 2 errors in this case.

### Conclusion

Schizophrenia is characterized by a load-dependent reduction in the centrality of the dPCC; this reduction relates to the severity of delusions that persist despite treatment. The centrality value of the dPCC under all working-memory loads fit an inverted U-shaped model, we found a left shift of this model distribution in patients with schizophrenia compared to healthy controls. This finding raises the question of whether noninvasive neuromodulation approaches that restore dPCC centrality in the presence of cognitive demands might have a distinct therapeutic effect on persistent positive symptoms (especially delusions) in schizophrenia.



**Acknowledgements:** The authors thank Sabrina D. Ford from Robarts Research Institute, Western University, for her assistance during the revision of the manuscript. The authors also thank all those who participated in this study.

**Affiliations:** From the Department of Psychiatry, Second Xiangya Hospital of Central South University, Changsha, Hunan, China (Wang, Xi, Liu, Deng, Zhang, Yang); the National Clinical Research Centre for Mental Disorders, Changsha, Hunan, China (Wang, Xi, Liu, Deng, Zhang, Yang); the Centre for Psychiatric Neuroscience, Feinstein Institutes for Medical Research, Manhasset, New York (Cao); the Division of Psychiatry Research, Zucker Hillside Hospital, Glen Oaks, New York (Cao); the Douglas Mental Health University Institute, Department of Psychiatry, McGill University, Montreal, Que. (Palaniyappan); the Department of Medical Biophysics, Western University, London, Ont. (Palaniyappan); the Robarts Research Institute, Western University, London, Ont. (Palaniyappan).

**Funding:** This work was supported by a grant from the National Natural Science Foundation of China (82071506 to Z. Liu), and the Natural Science Foundation of Hunan Province, China (2021JJ40884 to J. Yang). L. Palaniyappan acknowledges research support from the Tanna Schulich Chair of Neuroscience and Mental Health (Schulich School of Medicine, Western University) at the time of this study; the Monique H. Bourgeois Chair in Developmental Disorders (Douglas Research Centre, McGill University); and a salary award from the Fonds de recherche du Québec-Santé at the time of publication.

**Competing interests:** L. Palaniyappan reports royalties from Oxford University Press; consulting fees or honoraria from SPMM Course Limited, Janssen Canada, Otsuka Canada and the Canadian Psychiatric Association; and participation on an advisory board for Janssen Canada, all outside the submitted work. L. Palaniyappan is co-editor in chief of the *Journal of Psychiatry and Neuroscience*, but was not involved in the decision to review or accept the manuscript for publication. No other competing interests were declared.

**Contributors:** Z. Liu and J. Yang designed the study. M. Deng and W. Zhang acquired the data, which F. Wang, C. Xi, H. Cao and L. Palaniyappan analyzed. F. Wang, C. Xi, W. Zhang and J. Yang wrote the article, which Z. Liu, M. Deng, H. Cao and L. Palaniyappan reviewed. All authors approved the final version to be published, agree to be accountable for all aspects of the work and can certify that no other individuals not listed as authors have made substantial contributions to the paper.

**Data sharing:** The data that support the findings of this study are available on request from the corresponding author. The data are not publicly available because of privacy or ethical restrictions.

**Content licence:** This is an Open Access article distributed in accordance with the terms of the Creative Commons Attribution (CC BY-NC-ND 4.0) licence, which permits use, distribution and reproduction in any medium, provided that the original publication is properly cited, the use is noncommercial (i.e., research or educational use), and no modifications or adaptations are made. See: <https://creativecommons.org/licenses/by-nc-nd/4.0/>

## References

- Green MF, Nuechterlein KH. Should schizophrenia be treated as a neurocognitive disorder? *Schizophr Bull* 1999;25:309-19.
- Park S, Puschel J, Sauter BH, et al. Spatial working memory deficits and clinical symptoms in schizophrenia: a 4-month follow-up study. *Biol Psychiatry* 1999;46:392-400.
- Green MF, Kern R, Braff D, et al. Neurocognitive deficits and functional outcome in schizophrenia: are we measuring the "right stuff"? *Schizophr Bull* 2000;26:119-36.
- Niendam TA, Laird A, Ray K, et al. Meta-analytic evidence for a superordinate cognitive control network subserving diverse executive functions. *Cogn Affect Behav Neurosci* 2012;12:241-68.
- Menon V. Large-scale brain networks and psychopathology: a unifying triple network model. *Trends Cogn Sci* 2011;15:483-506.
- Callicott JH, Mattay VS, Bertolino M, et al. Physiological characteristics of capacity constraints in working memory as revealed by functional MRI. *Cerebral Cortex* 1999;9:20-6.
- Anticevic A, Cole MW, Murray JD, et al. The role of default network deactivation in cognition and disease. *Trends Cogn Sci* 2012;16:584-92.
- Van Snellenberg JX, Girgis RR, Horga G, et al. Mechanisms of working memory impairment in schizophrenia. *Biol Psychiatry* 2016;80:617-26.
- Thomas ML, Duffy JR, Swerdlow N, et al. Detecting the inverted-U in fMRI studies of schizophrenia: a comparison of three analysis methods. *J Int Neuropsychol Soc* 2022;28:258-69.
- Luo Q, Pan B, Gu H, et al. Effective connectivity of the right anterior insula in schizophrenia: the salience network and task-negative to task-positive transition. *Neuroimage Clin* 2020;28:102377.
- Hahn B, Harvey AN, Gold JM, et al. Load-dependent hyperdeactivation of the default mode network in people with schizophrenia. *Schizophr Res* 2017;185:190-6.
- Fryer SL, Woods SW, Kiehl KA, et al. Deficient suppression of default mode regions during working memory in individuals with early psychosis and at clinical high-risk for psychosis. *Front Psychiatry* 2013;4:92.
- Whitfield-Gabrieli S, Thermenos H, Milanovic M, et al. Hyperactivity and hyperconnectivity of the default network in schizophrenia and in first-degree relatives of persons with schizophrenia. *Proc Natl Acad Sci U S A* 2009;106:1279-84.
- Anticevic A, Repovs G, Barch D. Working memory encoding and maintenance deficits in schizophrenia: neural evidence for activation and deactivation abnormalities. *Schizophr Bull* 2013;39:168-78.
- Pu W, Luo Q, Palaniyappan L, et al. Failed cooperative, but not competitive, interaction between large-scale brain networks impairs working memory in schizophrenia. *Psychol Med* 2016;46:1211-24.
- Zhou L, Pu W, Wang J, et al. Inefficient DMN suppression in schizophrenia patients with impaired cognitive function but not patients with preserved cognitive function. *Sci Rep* 2016;6:21657.
- Farruggia MC, Laird AR, Mattfeld AT. Common default mode network dysfunction across psychopathologies: a neuroimaging meta-analysis of the n-back working memory paradigm. *bioRxiv* 2020 Jan 31. doi:10.1101/2020.01.30.927210
- Hahn B, Harvey A, Gold J, et al. Hyperdeactivation of the default mode network in people with schizophrenia when focusing attention in space. *Schizophr Bull* 2016;42:1158.
- Harrison BJ, Yücel M, Pujol J, et al. Task-induced deactivation of midline cortical regions in schizophrenia assessed with fMRI. *Schizophr Res* 2007;91:82-6.
- Yang J, Pu W, Wu G, et al. Connectomic underpinnings of working memory deficits in schizophrenia: evidence from a replication fMRI study. *Schizophr Bull* 2020;46:916-26.
- Pearson JM, Heilbronner SR, Barack DL, et al. Posterior cingulate cortex: adapting behavior to a changing world. *Trends Cogn Sci* 2011;15:143-51.
- Godwin D, Ji A, Kandala S, et al. Functional connectivity of cognitive brain networks in schizophrenia during a working memory task. *Front Psychiatry* 2017;8:294.
- Frydecka D, Eissa AM, Hewedi DH, et al. Impairments of working memory in schizophrenia and bipolar disorder: the effect of history of psychotic symptoms and different aspects of cognitive task demands. *Front Behav Neurosci* 2014;8:416.
- Krkovic K, Moritz S, Lincoln TM. Neurocognitive deficits or stress overload: why do individuals with schizophrenia show poor performance in neurocognitive tests? *Schizophr Res* 2017;183:151-6.
- Guimond S, Padani S, Lutz O, et al. Impaired regulation of emotional distractors during working memory load in schizophrenia. *J Psychiatr Res* 2018;101:14-20.
- Rubinov M, Sporns O. Complex network measures of brain connectivity: uses and interpretations. *Neuroimage* 2010;52:1059-69.
- Andreasen N. *Scale for the assessment of positive symptoms (SAPS)*. Iowa City (IA): University of Iowa; 1984.
- Andreasen N. The scale for the assessment of negative symptoms (SANS): conceptual and theoretical foundations. *Br J Psychiatry Suppl* 1989;(7):49-58.
- Gong Y, Wechsler D. *Adult Intelligence Scale (WAIS-CR) revision*. 2nd ed. Hunan, China: Hunan Press; 1992.
- Yan CG, Wang XD, Zuo XN, et al. DPABI: Data processing and analysis for (resting-state) brain imaging. *Neuroinformatics* 2016;14:339-51.

31. Yang GJ, Murray JD, Repovs G, et al. Altered global brain signal in schizophrenia. *Proc Natl Acad Sci U S A* 2014;111:7438-43.
32. Power JD, Barnes KA, Snyder AZ, et al. Spurious but systematic correlations in functional connectivity MRI networks arise from subject motion. *Neuroimage* 2012;59:2142-54.
33. Cortes C, Vapnik V. Support-vector networks. *Mach Learn* 1995; 20:273-97.
34. Tan W, Liu Z, Xi C, et al. Decreased integration of the fronto-parietal network during a working memory task in major depressive disorder. *Aust N Z J Psychiatry* 2021;55:577-87.
35. Leucht S, Samara M, Heres S, et al. Dose equivalents for second-generation antipsychotic drugs: the classical mean dose method. *Schizophr Bull* 2015;41:1397-402.
36. Fransson P, Marrelec G. The precuneus/posterior cingulate cortex plays a pivotal role in the default mode network: evidence from a partial correlation network analysis. *Neuroimage* 2008;42:1178-84.
37. Leech R, Braga R, Sharp DJ. Echoes of the brain within the posterior cingulate cortex. *J Neurosci* 2012;32:215-22.
38. Leech R, Kamourieh S, Beckmann CF, et al. Fractionating the default mode network: distinct contributions of the ventral and dorsal posterior cingulate cortex to cognitive control. *J Neurosci* 2011;31:3217-24.
39. Lamichhane B, Westbrook A, Cole MW, et al. Exploring brain-behavior relationships in the N-back task. *Neuroimage* 2020;212:116683.
40. Sormaz M, Murphy C, Wang HT, et al. Default mode network can support the level of detail in experience during active task states. *Proc Natl Acad Sci U S A* 2018;115:9318-23.
41. Spreng RN. The fallacy of a "task-negative" network. *Front Psychol* 2012;3:145.
42. Leech R, Leech R, Sharp DJ. Echoes of the brain within the posterior cingulate cortex. *J Neurosci* 2012;32:215-22.
43. Buckner RL, DiNicola LM. The brain's default network: updated anatomy, physiology and evolving insights. *Nat Rev Neurosci* 2019; 20:593-608.
44. Papez JW. A proposed mechanism of emotion. *J Neuropsychiatry Clin Neurosci* 1995;7:103-12.
45. Rolls ET. The cingulate cortex and limbic systems for emotion, action, and memory. *Brain Struct Funct* 2019;224:3001-18.
46. Whitfield-Gabrieli S, Ford JM. Default mode network activity and connectivity in psychopathology. *Annu Rev Clin Psychol* 2012;8:49-76.
47. Buckner RL, Andrews-Hanna JR, Schacter DL. The brain's default network. *Ann N Y Acad Sci* 2008;1124:1-38.
48. Margulies DS, Vincent JL, Kelly C, et al. Precuneus shares intrinsic functional architecture in humans and monkeys. *Proc Natl Acad Sci U S A* 2009;106:20069-74.
49. Zeharia N, Hofstetter S, Flash T, et al. A whole-body sensory-motor gradient is revealed in the medial wall of the parietal lobe. *J Neurosci* 2019;39:7882-92.
50. Tordesillas-Gutierrez D, Ayesa-Arriola R, Delgado-Alvarado M, et al. The right occipital lobe and poor insight in first-episode psychosis. *PLoS One* 2018;13:e0197715.
51. Yi HG, Leonard MK, Chang EF. The encoding of speech sounds in the superior temporal gyrus. *Neuron* 2019;102:1096-110.